

Dynamic Load Factor Estimation of a Typical Launch Vehicle during Atmospheric Phase

Stenny¹, Girish Babu P², S. Rajendran³, Dr. Rajesh P Nair⁴

¹PG Student, Dept. of Ship Technology, CUSAT, Kalamassery, Kerala

²Scientist/Engineer 'SF', SLRG/SLMD, VSSC, Thiruvananthapuram, Kerala

³ Scientist/Engineer 'G', Group Head, SRLG, STR, VSSC, Thiruvananthapuram, Kerala

⁴Assistant Professor, Dept. of Ship Technology, CUSAT, Kalamassery, Kerala

Abstract - A launch vehicle is exposed to various environments, during pre-launch and flight that must be considered for the design. As a launch vehicle travels through the atmosphere it may encounter turbulence / gusts or sudden control force demand. As the Length to Diameter ratio (L/D) of launch vehicles are generally more than 10, the effect of vehicle flexibility will be considerably high. The change in angle of attack and the elastic mode response can produce significant dynamic or flexible body loads. To design a launch vehicle, the structural loads are required to be estimated prior to the design. In the limit load estimation of launch vehicle, the combined rigid-body and flexible body loads are evaluated. For easiness, the total limit loads are expressed as the rigid-body load increased by a dynamic load factor (DLF) or flexibility factor (FF) to account for flexible body effects. Thus the work focuses on accurately estimating the flexible body loads for enveloping the limit loads for a launch vehicle due to sudden experience of gust, sudden application of control force and quasi-static flexibility, considering vehicle characteristics (frequency and mode shape). A finite element model of a typical launch vehicle (lift-off model) is modelled using beam elements. Free-free boundary condition is simulated since the vehicle loads are to be estimated during its flight conditions. A code is developed using MATLAB[®] for estimating the loads at the critical flight events. This code updates mass in the finite element models of launch vehicle at critical flight instances from the lift-off model, generates Aerodynamic & Control force data from pre-flight trajectory data and submits to finite element solver for extracting required results such shear force (SF), bending moment (BM), Mass and CG data of vehicle etc. Dynamic loads (SF and BM) caused by sudden gust and control force are estimated by Transient response analysis and loads for rigid body and quasi static bent shape are estimated by inertia relief method in MSC NASTRAN 2016. And these loads are compared with the rigid body load to accurately obtain the flexibility factor (= flexible body load / rigid body load *100). It is concluded from this study that the rigid body load is to be increased by flexibility factor of 15% to 53% due to the combined effect of gust, sudden application of control force and quasi-static flexibility together.

Key Words: Launch vehicle, Dynamic Load, Rigid body load, Flexible body load, Dynamic Load factor, Flexibility factor, Transient response, Gust, Control force, Quasi-static flexibility.

1. INTRODUCTION

A launch system consists of the launch vehicle, launch pad, and other infrastructure. A launch vehicle is exposed to various environments during pre-launch and its flight, and that must be considered for the design and safe operation of the system. These include conditions such as acoustic vibration, wind loading, and vibration due to engine thrust. These environments cause the launch vehicle to encounter forces that cause structural deformations and vibrations [1].

There are significant interactions between the atmosphere and the launch vehicle during the atmospheric phase. As a launch vehicle flies through the atmosphere, it may experience gusts. Gust consists of relatively short duration wind that changes a launch vehicle's wind induced angle of attack [1]. This change in the angle of attack occurs very fast so that the system's lower frequency vibration modes are excited. The angle of attack change and the elastic mode response can produce significant dynamic or flexible body loads. During powered ascent phase to maintain a controlled flight path of the vehicle, control force (side force) is to be generated by moving the thrust axis ("thrust vectoring"), usually with engine/motor gimbals or by varying the thrust of individual engines in a cluster. In order to maintain vehicle stability while flying through turbulence, the control system gimbals the engine [9] and subsequently generates control force. Beyond the local loads generated by the thrust vectoring devices, there are also dynamic loads on the vehicle due to the change in the thrust components along the longitudinal and lateral axes of the vehicle. These maneuvering loads are composed of low-frequency aerodynamic forces and the control or thrust-vectoring forces that steer the vehicle into the wind. These loads are significant only in the frequency range below 5 to 10 Hz [8]. Thus control force also exerts significant dynamic load on the vehicle. As the Length to Diameter ratio (L/D) of launch vehicles is generally more than 10, the effect of the quasi-static flexibility effect of the vehicle will be considerably high [14]. At given steady condition, aerodynamic force, control force and inertia force acting on the vehicle are bending it

and this quasi- static bent shape is also responsible for flexible body load by changing the local angle of attack. The magnitude of the aerodynamic loading will depend on the launch vehicle's speed, air density, total angle of attack, and the wind features through which the vehicle flies [3]. All vehicle motion and associated limit loads consist of rigid-body and flexible body response. For easiness, the total limit loads are expressed as the rigid-body load increased by a flexibility factor (FF) or dynamic load factor (DLF) to account for flexible body effects [13]. Evaluating the combined load with an augmentation in rigid-body load simplifies the analysis since rigid-body analyses do not need stiffness distributions, mode shapes, or frequencies.

For Flexible body loads during the atmospheric flight, analyses are typically performed at discrete times of flight (or Mach Numbers). Parameters that differ at the various times of flight are changes in finite element model, including the fluid levels in the launch vehicle tanks, tank pressures, remaining propellant in solid rocket motors and vehicle configuration. Critical load contributors that need to be considered include static-aero elastic loads (Aerodynamic load due to bent shape of the vehicle), atmospheric turbulence/gusts loads, buffet loads, control system-induced loads, thrust and thrust oscillation loads, drag loads, and jettison event loads [12].

Thus computation of rigid and flexible body loads on a launch vehicle is essential for the design and safe operation of the launch vehicle. For the present work, many critical flight events are analysed considering different Mach numbers & gust profiles and different rise-time for control force.

The Limit load is called as the maximum load experienced by vehicle during its service including rigid and flexible body loads. For each structure, Limit load is to be estimated for the structural design of the launch vehicle. An Ultimate load factor of 25% over the limit load will be used for structural design.

2. METHODOLOGY

1. The launch vehicle is idealized by beam elements and its Finite element model is made considering mass distribution, material, and geometric properties.
2. MATLAB code is developed for estimating the loads at the critical flight events. This code is used for updating the finite element models of the launch vehicle at critical flight instances from the lift-off model, generating force data (Aerodynamic force & Control force) and NASTRAN input deck file, submitting input deck to NASTRAN, extracting required results (SF, BM, Mass and CG data of the vehicle, etc.) from NASTRAN output.

3. Transient response analysis of NASTRAN is used for the dynamic load estimation due to gust and control force excitations. Rigid body loads and loads due to vehicle bent shape are estimated from the Inertia Relief method of NASTRAN.
4. All loads caused by gust, control force, and bent shape are added and compared with rigid body loads for flexibility factor estimation.
5. Computation of the flexibility factor at salient locations of vehicle length is done using Excel software.

3. NATURAL FREQUENCY AND MODE SHAPE ESTIMATION AT CRITICAL FLIGHT EVENTS

Dynamic analysis of a launch vehicle is used to determine the structure's response due to various excitations encountered during flight. It is related to the inertia forces developed by a structure when it is excited by dynamic loads applied suddenly [10]. Dynamic analysis for simple structure can be done manually, but for complex structures, finite element analysis can be used to calculate the frequencies and mode shapes [5].

3.1 Finite Element Model

The launch vehicle is idealized using beam elements with free-free boundary conditions as in flight. Modal characteristics of the launch vehicle like frequency, mode shape, etc. are generated through finite element analysis [4]. Fig-1 shows the finite element model of a typical launch vehicle using beam element, considering mass distribution, material, and geometric properties. It is modelled for free-free boundary condition.

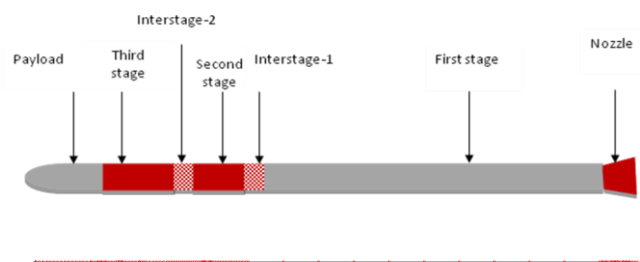


Fig-1: Finite Element Model of a Launch Vehicle

3.2 Natural Frequencies and Mode Shapes

The natural frequencies of a structure are the frequencies at which the structure tends to vibrate after a disturbance is removed. Modal Analysis is carried out to determine the natural frequency of the structure [10]. Natural frequencies and the corresponding modes are computed using normal mode analysis option (SOL 103) [4]. The first natural frequency of this typical vehicle is nearly 3 Hz.

The deformed shape of the structure at a specific natural frequency is termed its normal mode of vibration. Each natural frequency has a mode shape [6].

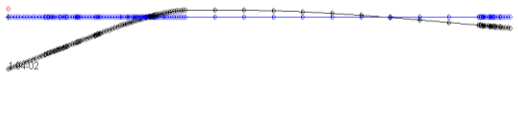
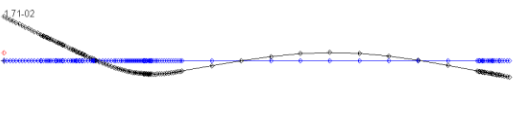
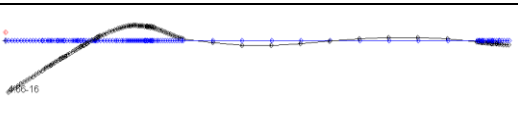
Natural frequencies and corresponding mode shapes are functions of the structural properties and boundary conditions. [4]. First Three Mode Shapes of the typical Launch Vehicle is shown in Table-1.

3.3 Critical Flight Events

Critical Flight events are the events that contribute to the maximum load on the launch vehicle during its flight in the atmospheric phase. Prior to the load estimation, the time instances at which the loads are to be estimated are to be decided. Following six instances are the critical flight events (M=0.8 to 6) considered for the present study, based on its significance:

1. Transonic condition (M = 0.8 to 1.2)
2. Maximum lateral Aero. load condition
3. Maximum lateral Aero. moment condition
4. Maximum dynamic pressure condition
5. Maximum control force condition
6. Maximum thrust condition

Table -1: First three bending frequencies and mode shapes

Modes	Mode shapes of Launch vehicle
I st mode	
II nd mode	
III rd mode	

Mach number and time instance of Critical Flight Events for loads estimated is given in Table-2. Maximum thrust force occurs at 87 sec which is beyond the atmospheric phase (> 30 km) [7]. Hence this event is not considered in the load estimation.

4. GUST EXERTED DYNAMIC LOAD ESTIMATION

Loads due to the rapidly changing wind features are referred to as turbulence and/or gust. The gust load analysis is performed to establish the vehicle's dynamic response to the gust that might be encountered in any flight. Transient

response analysis is the general approach for estimating forced dynamic response [4]. The analysis was carried out for all critical flight events. In the early days, sharp-edged and linear-ramp type gust profiles were used. Other types of synthetic gusts considered include the triangular, the trapezoidal, and the sine gusts. The two most common synthetic gust profiles used for launch-vehicle loads analysis are the Trapezoidal and One-minus-cosine profiles [2] as shown in Fig 3 & 4. Parameters that can be varied with these synthetic gust profiles include the amplitude and wavelength. The analysis is carried out for two profiles, viz., Trapezoidal and 1-Cosine gust profile for five critical events.

Table -2: Critical Flight Events for Loads estimated

Sl. No:	Critical Flight event	Mach Number	Time instance (sec)
1	Transonic condition	0.8	23
		1.1	29
		1.2	31
2	Maximum lateral Aerodynamic load condition	1.2	31
3	Maximum lateral Aerodynamic moment condition	1.2	31
4	Maximum dynamic pressure condition	1.6	41
5	Maximum control force condition	2.5	47
6	Maximum thrust condition	6.0	87

In the formulation of gust response, lateral aerodynamic force coefficient ($SdC_{N\alpha}/d_x$) is converted to concentrated aerodynamic force coefficient $SC_{N\alpha i}$.

$$\text{Lateral aerodynamic force for } i^{\text{th}} \text{ node} = SC_{N\alpha i} * q\alpha \text{ (N)} \quad (1)$$

From the aerodynamic force distribution data corresponding to each critical event, concentrated aerodynamic force is derived for all station points. Fig 2 shows the pictorial representation at Mach No: 1.2.

Trajectory data such as Mach number, dynamic pressure (q), relative velocity of the vehicle were taken from the pre-flight data. The analysis is accomplished by enveloping the vehicle in gust profiles aforementioned. Gust load input, finite element model update, and NASTRAN run for transient response analysis and output extraction are done using MATLAB code[15].

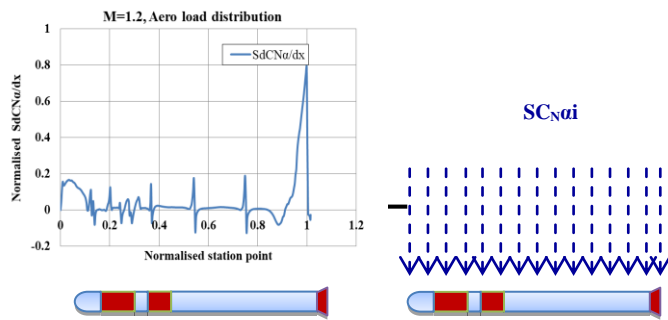


Fig-2: Representation of lateral aero. force coefficient distribution converted to concentrated values

• **Trapezoidal gust profile**

The launch vehicle is immersed in a trapezoidal gust profile with amplitude of 7m/s, and a gust wavelength of 300 m.

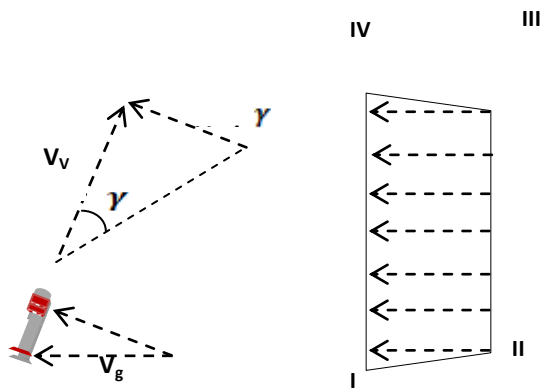


Fig 3: Launch Vehicle Immersed in a Trapezoidal Gust Profile

• **1-Cosine gust profile**

The amplitude and wavelength of the profile is defined as follows [11]:

$$\begin{aligned}
 V &= 0; & d < 0, d > 2d_m \\
 V &= (V_m/2)(1 - \cos(\pi d/d_m)); & 0 \leq d \leq 2d_m
 \end{aligned}
 \tag{2}$$

Where, V_m , gust magnitude = 7m/s

$$d_m, \text{ gust half-width} = 300/2 = 150 \text{ m}$$

d = distance in m

For the gust response study, this program generates gust models in the time domain for Trapezoidal and 1-Cosine gust profiles at various time instances at which FE models are generated. The program can be considered as a tool capable of generating the gust load input for launch vehicle. The output of this program updates the input file for NASTRAN (FE Software) and submits to NASTRAN software for transient response analysis to obtain the displacements, and accelerations of grid points, and forces in elements, at each output time step.

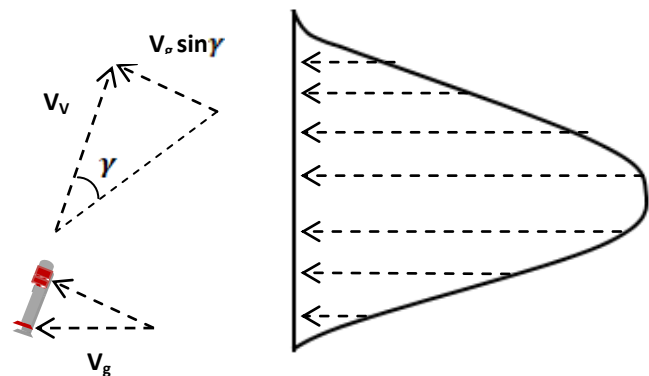


Fig-4: Launch Vehicle Immersed in a 1-Cosine Gust Profile

4.1 Gust Response

Transient response analysis is carried out at all critical flight events and important results obtained are Shear force (SF) and bending moment (BM) at all sub-structures of the vehicle. Typically displacements and accelerations at salient locations are also estimated.

The dynamic bending moment is obtained for all critical events from the above analysis for trapezoidal and 1-Cosine transient response analysis. Dynamic loads due to the Trapezoidal gust profile are more compared to the dynamic load due to 1-Cosine gust profile. Thus dynamic BM due to Trapezoidal gust profile is considered for the flexibility factor estimation.

5. CONTROL FORCE EXERTED DYNAMIC LOAD ESTIMATION

During powered ascent phase, the path of the vehicle is controlled by moving the thrust axis ("thrust vectoring"), usually with engine/motor gimbals or, by varying the thrust of individual engines in a cluster. The control system gimbals the engines to maintain vehicle stability while flying through turbulence.

Control force is applied as step force with a finite rise time as shown in Fig 5.

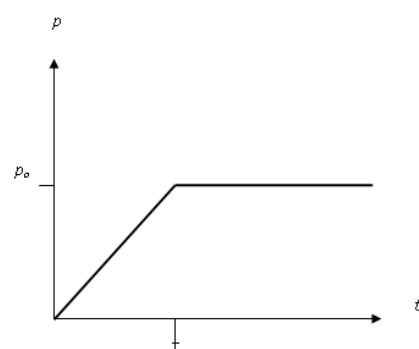


Fig -5: Control Force Applied as Step Force with Finite Rise Time

In reality, a force cannot be applied suddenly; it is of interest to consider a dynamic force that has a finite rise time, τ , but remains constant thereafter. The excitation has two phases: ramp or rise phase and constant phase [5].

$$p(t) = \begin{cases} p_o(t/\tau) & t \leq \tau \\ p_o & t \geq \tau \end{cases} \quad (3)$$

The frequency of the system is around 3 Hz; thus the time period is 0.33 sec.

5.1 Control Force Response

Transient response analysis is carried out at all critical flight events and important results obtained are Shear force (SF) and bending moment (BM) at all sub-structures of the vehicle. Typically displacements and accelerations at few salient locations are also estimated. Maximum acceleration (m/s^2) at the tip is 2.172 at 35 sec and 1.991 at 41 sec. And maximum deflection at tip is 0.0063 m at 35 sec and 0.0052 m at 41 sec.

6. QUASI STATIC BENT SHAPE CAUSED LOAD ESTIMATION

Aerodynamic force, control force and inertia forces bend the rocket due to its elasticity, which changes the aerodynamic load distribution due to varying angle of attack. The changed load distribution further bends the rocket, which causes a further change in loads.

$$\text{Lateral Aerodynamic force for } i^{\text{th}} \text{ node} = SC_{N_{ai}} * q (\alpha_r + \alpha_f) \quad (N) \quad (4)$$

Where $\{\alpha_r\}$ = Rigid body angle of attack at all station points

$\{\alpha_f\}$ = Angle of attack due to vehicle bending at all station points.

By equating the control moment and aerodynamic moment we get the trim control force required to counterbalance this aerodynamic moment as:

$$\text{Trim Control Force} = CF_{\text{Trim}} = \frac{FAT(X_{CG} - X_{CF})}{(X_{CF} - X_{CG})} \quad (5)$$

The trim control force is applied at X_{CF} . Total aerodynamic force (FAT) is acting at X_{cp} . The lift-off model with updated propellant mass is applied with aerodynamic and control force. Inertia relief analysis is carried out using NASTRAN software. Rigid body bending moment, shear force, deflection, and slope are extracted from the NASTRAN output.

And further, for estimation of flexible body loads, the slope along vehicle length or flexible body angle of attack is added to the rigid body angle of attack. Fig 6 shows the pictorial representation of the incremental increase in angle of attack due to the quasi-static flexibility effect.

6.1 Quasi-static Bend Shape

Inertia relief analysis is carried out and the deflections and loads are obtained for all critical flight events. Rigid body and flexible body deflections are plotted for Transonic condition (Time =35 sec). From Fig 7, it is clear that deflection is augmented due to the quasi-static flexibility effect. Rigid body

and flexible body bending moment and shear force are obtained from the inertia relief method.

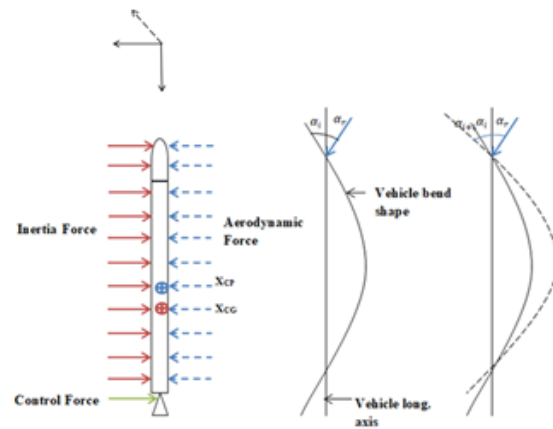


Fig -6: Increase in angle of attack due to Quasi-Static Flexibility Force

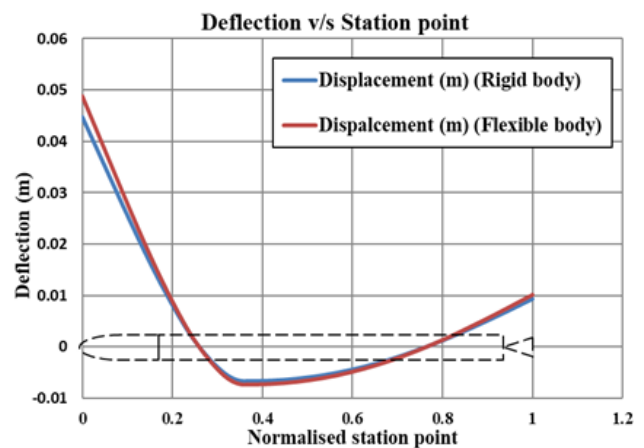


Fig -7: Rigid Body and Flexible body Deflection (Transonic)

7. RESULTS AND DISCUSSIONS

7.1 Results

The dynamic lateral loads (SF & BM) due to Gust load (Trapezoidal and 1-Cosine gust) and Control force, and lateral loads due to quasi-static flexibility are evaluated for all critical events. And these loads are compared with the rigid body load to accurately obtain the flexibility factor (= flexible body load / rigid body load *100). It can be inferred from the above analysis and results that a significant augmentation is seen in the lateral loads. Incremental loads are summed up, and the percentage over rigid body loads is estimated to get the total flexibility factor along the vehicle length. Table 3 gives the individual flexibility factors contributed by gust, sudden control force and quasi-static bent shape. Table 4 gives the total flexibility factors, considering all effects. Here rigid body load value is taken as 100% at the respective location and flexibility factor to be considered over rigid body load is given.

Table 3 Flexibility Factor break-up for each load case

Critical Event	Sub-system	Flexible body BM %		
		Gust	Control force	Quasi-static bent shape
23 sec (Transonic)	Payload Fairing - AE	4.1	0.3	4.1
	Interstage-2, FE	19.9	1.2	4.1
	Interstage- 1, AE	34.7	1.4	4.1
29 sec (Transonic)	Payload Fairing - AE	4.5	1.6	7.0
	Interstage-2, FE	21.9	6.0	7.1
	Interstage- 1, AE	38.0	7.9	7.2
31 sec (Max Lateral Aero. load)	Payload Fairing - AE	3.4	1.5	8.2
	Interstage-2, FE	16.3	6.1	8.3
	Interstage- 1, AE	26.6	8.1	8.4
41 sec (Q max)	Payload Fairing - AE	4.2	1.2	9.4
	Interstage-2, FE	12.3	4.8	9.4
	Interstage- 1, AE	18.1	6.3	9.5
47 sec (CF max)	Payload Fairing - AE	4.3	2.3	8.2
	Interstage-2, FE	12.7	8.4	8.3
	Interstage- 1, AE	20.9	11.2	8.3

Table 4 Total Flexibility Factor for each load case

Critical Event	Sub-system	Total Flex factor (%)
23 sec (Transonic)	Payload Fairing - AE	8.5
	Interstage-2, FE	25.2
	Interstage- 1, AE	40.3
29 sec (Transonic)	Payload Fairing - AE	13.2
	Interstage-2, FE	35.1
	Interstage- 1, AE	53.1
31 sec (Max Lateral Aero. load)	Payload Fairing - AE	13.2
	Interstage-2, FE	30.7
	Interstage- 1, AE	43.2
41 sec (Q max)	Payload Fairing - AE	14.9
	Interstage-2, FE	26.6
	Interstage- 1, AE	33.9
47 sec (CF max)	Payload Fairing - AE	14.8
	Interstage-2, FE	29.4
	Interstage- 1, AE	40.4

Fig 8 Shows the bar chart representing the load augmentation at transonic condition (M=1.2).

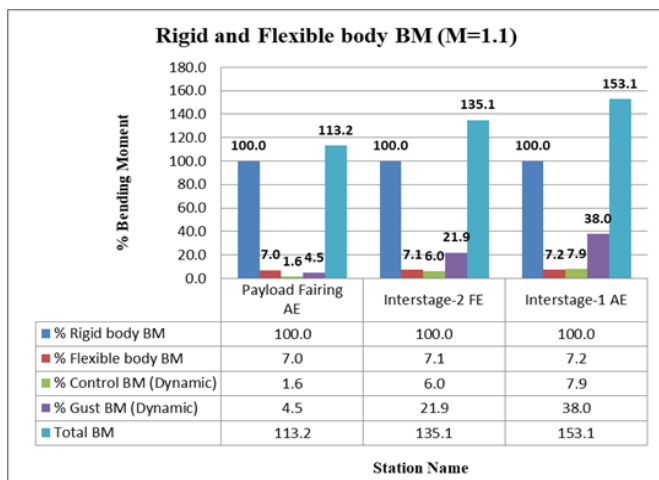


Fig -8 : Load augmentation due to flexible loads (M=1.2) at 29 sec

The Pie chart shows, the total rigid body loads due to aero, control (100%) and the break-up of flexible body loads due to gust, control and quasi-static bending for transonic event.

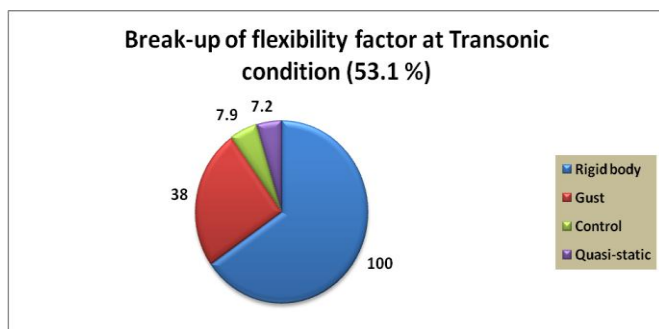


Fig -9: Rigid body loads and the break-up of flexible body loads

From the load results, it can be inferred that vehicle flexibility increases the lateral loads significantly. The maximum load augmentations over rigid body load due to the above-mentioned phenomena are given below:

- Sudden experience of gust = 4.5 to 38 % of rigid body loads along the length
- Sudden application of control force = 2.3 to 11.2 % of rigid body loads along the length
- Quasi-static flexibility = 4.1 % to 9.5% of rigid body loads along the length

7.2 Discussions

It is observed that the gust excitation causes more dynamic loads, as expected. Quasi-static bending loads follow it. The control force effect is seen more towards the aft ward portion of the vehicle only.

Initially, we assumed a 50% flexibility factor at all events. Now we will be using realistic values along the length at various events. Thus the total incremental loads are summed

up, and the percentages over rigid body loads are estimated to get the total flexibility factor as 15% - 53%. And thereby the lateral loads are accurately enveloped considering the rigid body and flexible body loads.

8. CONCLUDING REMARKS

A launch vehicle is subjected to different environments during pre-launch and during its flight. In the present work, launch vehicle loads during flight alone is considered. During vehicle motion, loads consist of two parts, namely rigid-body load and flexible-body load. Previously, the combined rigid-body load and flexible-body load was estimated by augmenting the rigid-body load by a flexibility factor (FF) or dynamic load factor (DLF) to account for flexible -body effects. Evaluating the combined load (Limit load) by this method simplifies the load analysis since rigid-body analysis does not need stiffness distributions, mode shapes, or frequencies.

During the atmospheric flight, five critical flight events ranging from M=0.8 to 2.5 are considered for load estimation. Flexible body loads are estimated at all critical flight events due to sudden gust experience, sudden application of control force and quasi-static bent effect. From the load results, it can be inferred that flexibility increases the lateral load significantly. The maximum load augmentations over rigid body load due to above-mentioned phenomena are given below:

Sudden experience of gust = 4.5 - 38 % of rigid body loads

Sudden application of control force = 2.3 - 11.2 % of rigid body loads

Quasi-static flexibility = 4.1 to 9.5% of rigid body loads.

Thus, the total incremental loads are summed up, and the percentages over rigid body loads are estimated to get the total flexibility factor as 15% - 53%, instead of a constant 50%. And thereby the lateral loads are accurately enveloped considering the rigid body and flexible body loads.

REFERENCES

- [1] Kabe, A. M., & Kendall, R. L. (2010). Launch Vehicle Operational Environments. Encyclopaedia of Aerospace Engineering.
- [2] Collins, D. F., & Morgan, H. G. (1963). Some applications of detailed wind profile data to launch vehicle response problems. AIAA Journal, 1(2), 368-373
- [3] Lester, H. C., & Tolefson, H. B. (1964). A study of launch-vehicle responses to detailed characteristics of the wind profile. Journal of Applied Meteorology, 3(5), 491-498
- [4] MSC Software (2016). MSC Nastran 2016 dynamic analysis user's guide.
- [5] Chopra, A. K. (2017). Dynamics of structures. Theory and applications to Earthquake Engineering
- [6] Harris, C. M., & Piersol, A. G. (2002). Harris' shock and vibration handbook (Vol. 5). New York: McGraw-Hill

- [7] Appleby, B. A., Martin, J. D., & Schuett, R. H. (1966). Dynamic loads analysis of space vehicle systems-Launch and exit phase.
- [8] Kern, D. L. (2001). Dynamic Environmental Criteria. National Aeronautics and Space Administration, NASA-HDBK-7005.
- [9] Dotson, K. W., & Tiwari, S. B. (1996). Formulation and analysis of launch vehicle maneuvering loads. *Journal of spacecraft and rockets*, 33(6), 815-821.
- [10] Wijker, J. J. (2004). *Mechanical vibrations in spacecraft design*. Springer Science & Business Media.
- [11] Adelfang, S. I., & Smith, O. (1998, January). Gust models for launch vehicle ascent. In *36th AIAA aerospace sciences meeting and exhibit* (p. 747).
- [12] Lustig, M. (2017). *Modeling of Launch Vehicle during the Lift-off Phase in Atmosphere* (Doctoral dissertation, Czech Technical University in Prague).
- [13] Vause, R., & Starr, B. (2011, August). Trajectory-Based Loads for the Ares IX Test Flight Vehicle. In *AIAA Atmospheric Flight Mechanics Conference* (p. 6463).
- [14] Lukens, D. R., Schmitt, A. F., & Broucek, G. T. (1961). Approximate transfer functions for flexible-booster-and autopilot analysis (No. AE-61-0198). General dynamics corp pomona ca pomonadiv.
- [15] MATLAB[®] 2014 product documentation